

Condensation in continuous stochastic mass transport models

Christos Christou and Andreas Schadschneider

Institute for Theoretical Physics, University of Cologne, Zùlpicher StraÙe 77, D-50937 Kùln, Germany

(Dated: May 6, 2022)

We study the dynamics of condensation for a stochastic continuous mass transport process defined on a one-dimensional lattice. We use an extreme value approach in order to describe the properties of the system in the thermodynamic limit. Furthermore we discuss the properties of finite size systems where three different variations of the truncated random average process will be presented. We generalize hereby the regular truncated process by introducing a new parameter γ and derive a rich phase diagram in the $\rho - \gamma$ plane where several new phases next to the condensate or fluid phase can be observed.

I. INTRODUCTION

Condensation is a phenomenon occurring in a plethora of physical systems and through several realizations. The most prominent example is the Bose-Einstein Condensation [1]. In statistical physics the notion of condensation is widely used to describe any process in which a finite fraction of some conserved quantity becomes localized in the phase space. In this context there has been an increasing interest in condensation transitions arising out of equilibrium observed in a variety of works in fields as diverse as traffic models [2–4], quantum gravity [5], networks [6, 7], economics [8, 9], granular materials [10], and mass transport [11, 12]. It is important to note here that many of these different instances of condensation share common and basic features. The analysis of these properties advanced greatly in the last years through the study of driven diffusive systems and, in particular, of the zero-range process (ZRP) or variants of it [13, 14].

Our goal in this paper is to expand this study to a substantially diverse manifestation of the stochastic mass transport process. In the usual contexts mentioned above, condensation is a phenomenon observed for systems evolving in a countable state space. Here we are concerned with the condensation transition occurring in continuous stochastic mass transport models such as the random average process (RAP). RAP can be grasped as a continuous variant of the zero-range process (ZRP) where instead of particle configurations we are engaged with the distribution of continuous variables, which we will call masses. Processes taking place in a continuous phase space setting have served as a basic model for a variety of physical systems and therefore have been the object of a large number of studies in the last years [15–23]. We have to note here that they also provide an interesting challenge since in contrast to processes with a countable state space the existence of a unique stationary measure is not given [25–27] allowing us thus to study systems with broken ergodicity [28].

Furthermore the metastability and phase transition properties related to the condensation phenomenon which became recently an object of scientific interest [29] are easily implemented in a continuous phase space setting. These features are not strictly associated with

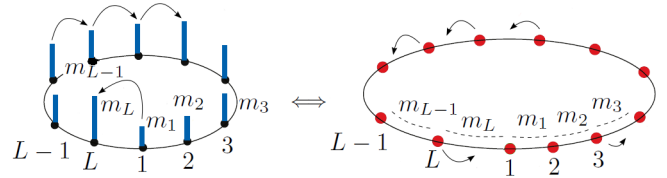


FIG. 1. Equivalence between the particles on a circle and mass exchange sites picture for the asymmetric random average process

the traditional zero-range process but require artificially complex dynamics which are often relevant for different practical applications. In order to realize these different complex processes we will use a fraction density, ϕ , formalism. For most of these models a large deviation theory approach proves to be insufficient. Fortunately rigorous and useful results related to this transition can be derived by analyzing the extreme value distribution of the system.

The remainder of this paper is organized as follows. In the next section we will briefly introduce the random average process. We will describe hereto the master equation for the free asymmetric random average process and discuss some relevant properties arising from the corresponding factorizable single site mass distribution. In Sec III we will evaluate the extreme value properties of this distribution and discuss the implications for the thermodynamic limit. In Sec IV we will present and analyze three different cases of a local fraction density, associated with the truncated asymmetric random average process (TARAP), zero-range random average process (ZRRAP) and the shortened random average process (SRAP). The last section is reserved for our final remarks.

II. MODEL

The random average process is a stochastic mass transport system defined on a lattice Λ_L of L sites, which we fix to be one-dimensional with periodic boundary conditions. This picture is equivalent to that of a particle

system defined on a ring as shown in Figure 1. Configurations are denoted by $\mathbf{m}(t) = \{m_k(t) : k \in \Lambda_L, t \in \mathbb{N}\} \in \mathcal{M}_L$ where $m_k(t) \in \mathbb{R}$ is the mass at site $k \in \Lambda_L$ at the time point t . Each mass can be arbitrarily large and the state space is hereby given by $\mathcal{M}_L = \mathbb{R}_+^{\Lambda_L}$. In the following we use for the stationary values the notation $m_i = \lim_{t \rightarrow \infty} m_i(t)$.

We consider here parallel update dynamics where at each discrete time step a random vector $\mathbf{r}(t) = \{r_k(t) : k \in \Lambda_L, t \in \mathbb{N}\}$ with $r_i(t) \in [0, 1]$ is generated from a probability density function ϕ which is called *fraction density*. The fraction $r_i(t)$ determines the amount of mass $r_i(t)m_i(t)$ chipped off from site i . For totally asymmetric processes the chipped off mass is transported to one neighboring site (we choose here the direction $i \rightarrow i + 1$). The process is therefore described by the master equation

$$m_i(t) = (1 - r_i(t-1))m_i(t-1) + r_{i-1}(t-1)m_{i-1}(t-1). \quad (1)$$

In the past several rigorous results for state-independent fraction densities have been derived [30–34]. The simplest version of the asymmetric random average process (ARAP) is given for a constant fraction density $\phi(r|m) = \text{const.}$ This process is described often as free ARAP since no restriction except the conservation of the total mass, $M = \sum_i m_i(t) = \rho L$, is applied.

As shown in [35] the steady state distribution of mass transport processes factorizes if the fraction density is given by a relation of the form

$$\phi(r|m) \propto v(r)u(m - rm). \quad (2)$$

For this fraction density we have a stationary state described by the mass distribution

$$P(m_1, \dots, m_L) = \frac{\prod_{i=1}^L f(m_i)}{Z(M, L)} \delta\left(\sum_{i=1}^L m_i - M\right) \quad (3)$$

where the function $f(m)$ is given by

$$f(m) = \int_0^m dr m v(r) u(m - rm) \quad (4)$$

and the "canonical partition function" is just the normalization

$$Z(M, L) = \prod_{i=1}^L \int_0^\infty dm_i f(m_i) \delta\left(\sum_{i=1}^L m_i - M\right) \quad (5)$$

We have to note here that $P(m_1, \dots, m_L)$ is equivalent to the probability of picking L independent and identically distributed random variables from a common distribution $f(m)$, conditioned on the fixed value of their total sum. This allows us to verify our analytical results by using a Monte Carlo simulation where we create L independent and identically distributed random variables, $\tilde{m}_i \forall i \in \mathbb{Z} \cap [0, L]$, with the single-site mass distribution

$$p(\tilde{m}) = f(\tilde{m}) \frac{Z(\rho L - \tilde{m}, L - 1)}{Z(\rho L, L)} \quad (6)$$

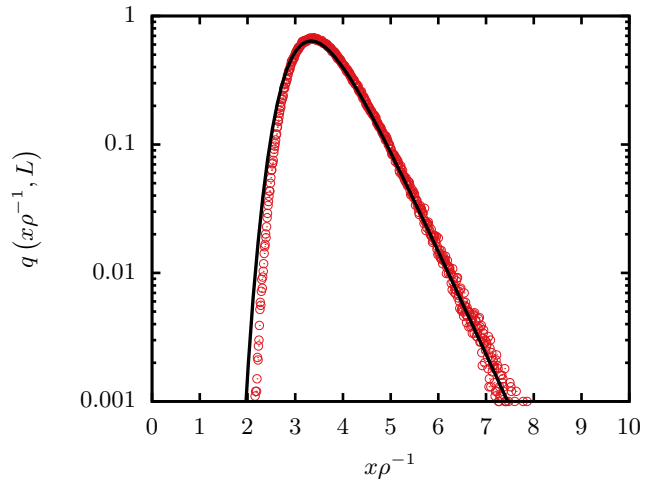


FIG. 2. Numerical (red circles) and analytical (black line) derivation of the largest value distribution for a free ARAP system with $L = 100$ and $\rho = 1$.

and normalize them by their sum

$$m_i = \frac{\rho L \tilde{m}_i}{\sum_{i=1}^L \tilde{m}_i}. \quad (7)$$

By comparing this method with the more time consuming one, where different initial configurations were evolved according to the update rules derived from the master equation (1), we can observe an excellent agreement.

III. EXTREME VALUE THEORY

For general fraction densities (2) is not fulfilled and a factorization of the corresponding partition function is impossible. Consequently the usual relation for the critical density of the system

$$\rho_c = \int dm m f(m) \quad (8)$$

cannot be applied here. It seems impossible to derive an analytical expression for ρ_c in the special case of mass exchange processes with truncation mechanics and we have to rely on numerical simulations in order to produce a phase diagram. Nevertheless the equations presented in this section will help us to understand the conditions under which a condensation may take place.

In the following we prefer to consider the order statistics $\{\ell_k(t)\}$ instead of the mass configuration $\{m_i(t)\}$. Hence we use the notations $\ell_k(t)$ with

$$\ell_L(t) < \ell_{L-1}(t) < \dots < \ell_1(t) = \max_{1 \leq i \leq L} m_i(t) \quad (9)$$

in order to describe the k -largest mass at the time-point t in the system.

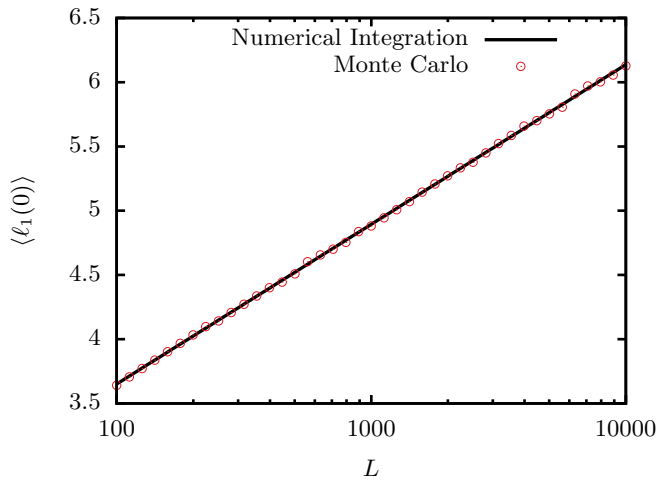


FIG. 3. Mean largest value for different lengths in the special case of $\rho = 1$. Each data point was calculated by averaging over 10^4 different Monte Carlo simulations.

Usually truncation processes as the ones presented in Sec. IV are defined by a cutoff parameter, Δ , according to which the dynamics of the process are specified. We choose here to set $\Delta = 1$. This of course does not lead to a loss of generality since the dynamics of the process

are fully specified by the extreme value statistics which are given only by the density and length of the system.

For all systems considered in this paper we follow the free ARAP update rules as long as $\ell_1(t) < 1$ (or $\ell_L(t) > 1$ correspondingly). It is therefore logical to set the initial distribution of the system equal to the steady state distribution of the free ARAP, which has the single-site mass distribution

$$p(m) = \frac{4m}{\rho^2} \exp\left(-\frac{2m}{\rho}\right). \quad (10)$$

Then we know from [36] that the probability of $\ell_1(0) \leq x$ is given by

$$P(x, M, L) = \frac{I(x, M, L)}{Z(M, L)} \quad (11)$$

where

$$I(x, M, L) = \prod_{i=1}^L \int_0^x dm_i f(m_i) \delta\left(\sum_{i=1}^L m_i - M\right) \quad (12)$$

and $Z(M, L)$ is given by $Z(M, L) = I(\infty, M, L)$ (see equation (5) above).

The critical mass for a condensation phase transition of the free ARAP is infinite and we can apply a saddle point approximation in order to calculate the exact expression of Eq. (11)

$$P(x, M, L) = \frac{\int_{c-i\infty}^{c+i\infty} ds \exp L(\rho s - 2 \ln s) - \exp L[\rho s - 2 \ln s + \ln(1 - e^{-sx} - xse^{-sx})]}{\int_{c-i\infty}^{c+i\infty} ds \exp L(\rho s - 2 \ln s)} \quad (13)$$

or equivalently

$$P(x\rho^{-1}, L) = \exp\left[-L\left(\frac{2x}{\rho} + 1\right)e^{-\frac{2x}{\rho}}\right]. \quad (14)$$

In the following calculations the probability distribution function

$$q(x\rho^{-1}, L) = \rho \frac{\partial}{\partial x} P(x\rho^{-1}, L) \quad (15)$$

will be useful.

Based on these formulas we can calculate the mean largest value

$$\frac{\langle \ell_1(0) \rangle}{\rho} = - \sum_{n=1}^{\infty} \binom{-L}{n} \frac{1}{2n} \sum_{k=0}^n \frac{n^k}{k!}. \quad (16)$$

The behavior shown in Figure 3 is best approximated by the function

$$\langle \ell_1(0) \rangle = 0.54\rho \ln(8.63L + 1). \quad (17)$$

We have to note here that the position of the largest value in the system is neither stable nor does it perform a continuous drift but shows irregular jumps. It is therefore appropriate to speak about a resetting of the largest value to a random position constantly during the evolution of the system. Due to this resetting it is important to calculate the distribution of the second largest value in order to describe the properties of the transition $\{\ell_{1,t} > 1\} \leftrightarrow \{\ell_{1,t+1} < 1\}$.

We start therefore by the formula

$$\Pr\{\ell_2(0) < x\} = \Pr\{\ell_1(0) < x\} + \Pr\{\ell_2(0) < x < \ell_1(0)\}. \quad (18)$$

Since the term $\Pr\{\ell_{1,0} < x\}$ has been calculated above we concentrate now on the second term [37]

$$\Pr\{\ell_2(0) < x < \ell_1(0)\} = L \int_x^{\infty} dm_1 f(m_1) \times \frac{\prod_{i=2}^L \int_0^x dm_i f(m_i) \delta\left(\sum_{i=2}^L m_i - M\right)}{\prod_{i=1}^L \int_0^{\infty} dm_i f(m_i) \delta\left(\sum_{i=1}^L m_i - M\right)}. \quad (19)$$

In order to evaluate this expression we use a saddle point

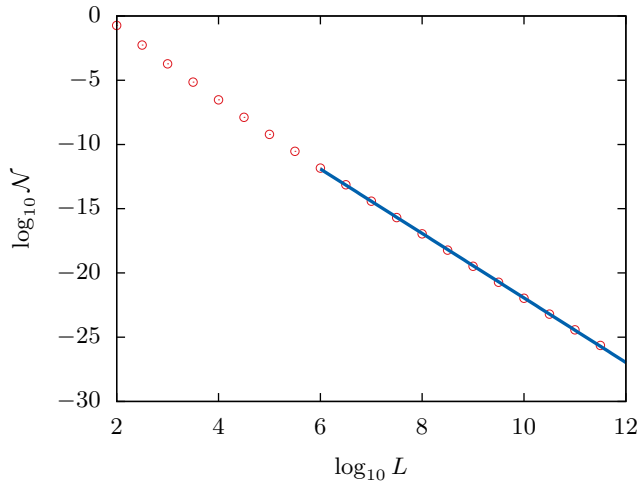


FIG. 4. Total probability $\mathcal{N} = \int d\rho \Pr \{\ell_{2,0} < 1 < \ell_{1,0}\}$ vs the length of the system L . We find out that for increasing lengths this weight tends to zero with an algebraic law. Numerically we find $\mathcal{N} \propto L^{-2.5}$ for $L \rightarrow \infty$.

approximation of the inverse Laplace transform by determining the minimum of the function

$$h(s) = \rho s + \frac{1}{L} \ln \int_x^\infty dm f(m) e^{-sm} + \frac{L-1}{L} \ln \int_0^x dm f(m) e^{-sm}. \quad (20)$$

We can deduce with (20) that

$$\lim_{L \rightarrow \infty} \Pr \{\ell_{2,0} < x < \ell_{1,0}\} = 0 \quad (21)$$

which correspondingly leads to

$$\lim_{L \rightarrow \infty} \Pr \{\ell_2(0) < x\} \sim \lim_{L \rightarrow \infty} \Pr \{\ell_1(0) < x\}. \quad (22)$$

This is expected since the configuration space of the largest value increases only with $\ln L$ while the number of sites increases with L leading therefore to a degenerate distribution. This feature is reflected in Figure 4 where the total probability

$$\mathcal{N} = \int d\rho \Pr \{\ell_2(0) < 1 < \ell_1(0)\} \quad (23)$$

is shown as function of the length of the system.

On the other side if we consider the density ρ^* for which the expression $\Pr \{\ell_2(0) < 1 < \ell_1(0)\}$ is maximal,

$$\frac{d}{d\rho} \Pr \{\ell_2(0) < 1 < \ell_1(0)\} |_{\rho^*} = 0, \quad (24)$$

we see in Figure 5 that the behavior of the function $\rho^*(L)$ is described by a monotone decreasing function for increasing lengths. These results confirm the broken ergodicity picture first assumed in [28]. In detail we show that for sufficiently high densities ($\rho > (\ln L)^{-1}$) in the thermodynamic limit we arrive at a state where a macroscopic number of sites have a mass above 1. In this case

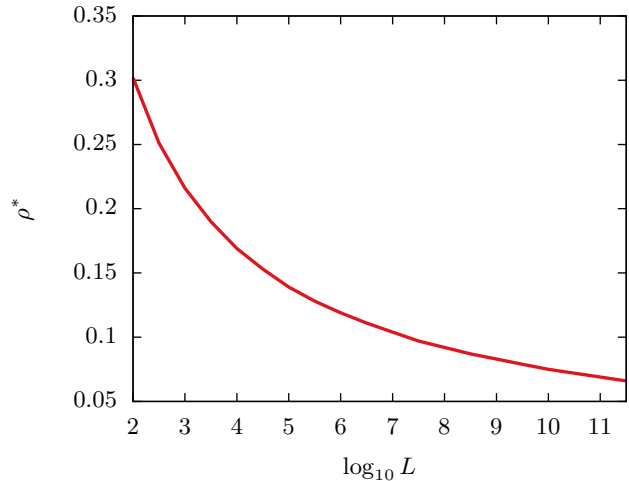


FIG. 5. Density ρ^* as function of the length of the system.

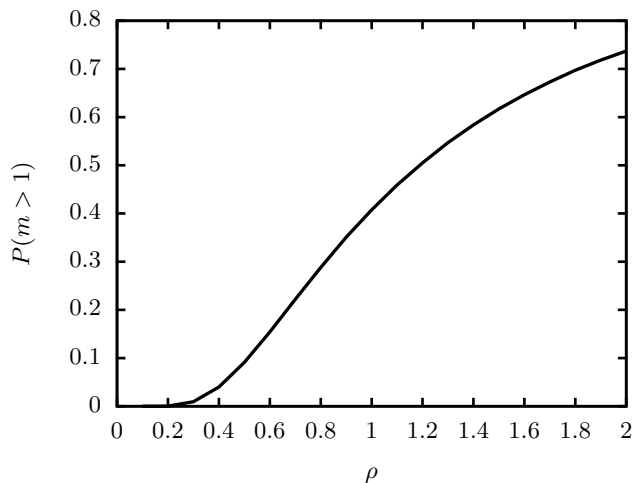


FIG. 6. Proportion of masses for a free ARAP consisting $L = 100$ sites with a value above 1. We see that $P(m > 1) > 0.5$ for $\rho = 1.2$.

we have almost surely a condensate in the system with an infinite lifetime. Similarly for $\rho \ll (\ln L)^{-1}$ we almost surely can observe states with $\ell_{1,t} < 1$ and a vanishing transition probability $\{\ell_1(t) < 1\} \rightarrow \{\ell_1(t+1) > 1\}$ for $L \rightarrow \infty$ and $\forall t \in \mathbb{N}$.

Before we proceed to the study of systems with finite length it is important to give an expression for the proportion of sites with a mass above the threshold of 1 for a specific density value. This function is shown in Fig. 6 and is given by the function

$$\Pr \{m > 1\} = \left(\frac{2}{\rho} + 1 \right) e^{-\frac{2}{\rho}}. \quad (25)$$

IV. TRUNCATED PROCESSES

In the following we use the term truncation in order to describe in general processes for which the expected transported mass per site and time-point is below 50% under certain conditions¹. We will consider here the special case where the dynamics of the system depend on the actual configuration $m_t = (m_{1,t}, \dots, m_{L,t})$. The universal form can be written as $\phi = \phi(r_{1,t}, \dots | m_{1,t}, \dots)$. The simplest case for such a system (and inspiration for this paper) is described by a process for which the fraction of transported mass is set to zero if the overall transported fraction is bigger than 1 ($rm > 1$) [28].

We start now with the analysis of truncation processes with a finite length. This is a yet unstudied but very interesting subject since many realizations of physical systems induce truncated behavior. Hereby one has to consider next to the probability of the condensate transition also the stability of those condensates. Unfortunately an analysis of this property proves to be difficult, if not impossible. In order to avoid this problem we decided to introduce a parameter γ which allows us to control the persistence of a condensate in the system. The effect of this parameter can be read from the corresponding fraction densities presented in the following three subsections.

A. TARAP

We start by the case of the truncated random average process (TARAP) where each rate, $r_i(t)$, is independently and identically uniformly distributed in the interval $[0, 1]$, but set to zero if the transported mass $r_i(t)m_i(t)$ exceeds a certain cutoff (which we choose to be 1 as explained in Section III).

The corresponding fraction density $\phi = \prod_i \phi(r_i(m_i))$ is given by

$$\phi(r|m) = [1 - R(m)]\delta(r) + \Theta(R(m) - r), \quad (26)$$

where Θ is the Heaviside step-function and

$$R(m) = \min \{1, m^{-\gamma}\} \quad (27)$$

represents the maximum possible fraction. For $\gamma = 1$ the fraction density of the original TARAP [28] is restored. The weight function of this distribution is given by

$$f(m) = \int_0^m d\tilde{m} \int_0^1 dr \phi(r|\tilde{m}) = m \quad (28)$$

¹ This definition deviates from the usual one associated with processes for which the transported fraction of mass is finite even in the thermodynamic limit.

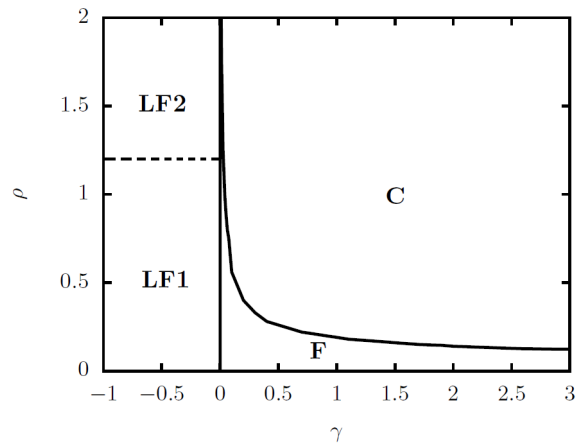


FIG. 7. Phase diagram for the TARAP model in the ρ - γ plane for $L = 100$. The dashed line does not correspond to a phase transition but describes the crossover between **LF1-LF2**.

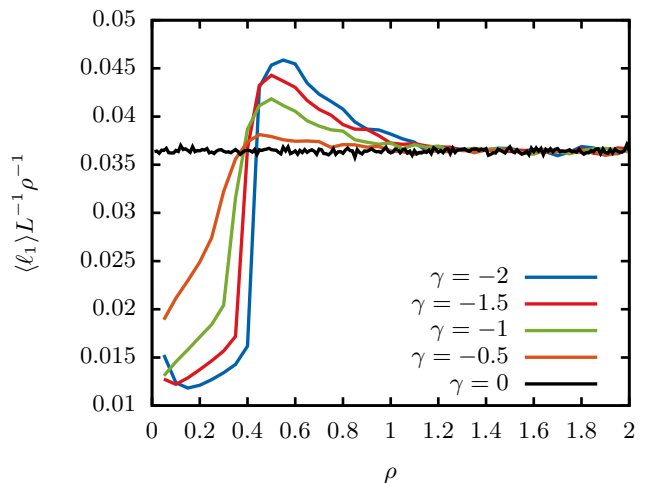


FIG. 8. Mean largest value of the TARAP in the stationary limit for $L = 100$ and different values of γ .

and the moments of this density are given by the equation

$$\mu_k = \frac{1}{f(m)} \int_0^1 dr r^k m^{k+1} \phi(r|m) = \frac{m^k R^{k+1}(m)}{k+1}. \quad (29)$$

By using a Monte Carlo simulation one can observe three different phases as represented in Figure 7. We characterize these phases by the distribution of the parameter $\langle \ell_1(T) \rangle \rho^{-1} L^{-1}$ averaged over 10^5 realizations in the stationary regime. We have to note here that since it is impossible to define analytically the time necessary for the distribution to become stationary, a numerical method becomes indispensable. For most of the parameter sets $\{\rho, \gamma\}$ and $L = 100$ a running time of $T = 10^5$ is sufficient.

For $\gamma < 0$ we see that the flux of the system is below the free ARAP expectations and the overall variance of

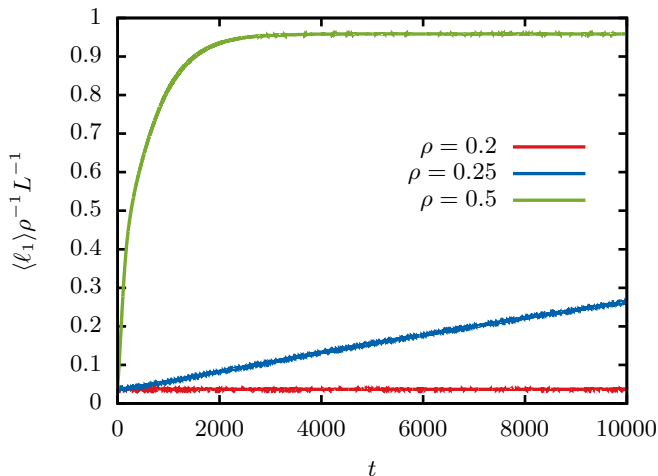


FIG. 9. Time evolution of the largest mass for the TARAP for $L = 100$, $\gamma = 1$ and different densities.

the single site mass distribution is also minimal. We characterize therefore this phase as low-flow phase (**LF**). In this phase for small densities the mean largest value of the system is below the characteristic $0.54\rho \ln(864) = 3.65\rho$ (see Eq. (17)) as calculated for the free ARAP case. This feature changes completely for higher densities ($\rho \approx 0.4$ for $\gamma = -1$), where we observe values of ℓ_1 well above the free ARAP expectation. We see that in this case the truncation has a significant effect on the distribution of the largest value (**LF1**).

For increasing densities ($\rho > 1.2$) the order parameter ℓ_1 shows no difference to the free ARAP case as shown in Figure 8. For such high densities more than half of the sites have a mass below 1 and the effect of the truncation in the distribution of the largest value becomes negligible. At the same time this state cannot be described as fluid since the flux in the system is well below $\frac{\rho}{2}$ (**LF2**). We have to note here that we still lack a complete understanding of the dynamics for $\gamma < 0$. A first step in this direction consists in the study of the system for $\gamma = -\infty$ which will be analyzed in detail in a following paper.

For $\gamma > 0$ we can observe two different phases. For small values of γ the differences to the free ARAP system are minimal. This phase is often characterized as fluid phase (**F**). The probability of condensation as well as the lifetime of the corresponding condensates are small in this phase and consequently no deviation from $\langle \ell_1 \rangle = 0.54 \ln(8.63L + 1)$ could be observed in our simulation.

For high densities and values of γ we are in the condensate phase (**C**). In this phase several condensates may appear in the system and a steady increase of the largest value can be observed for high values of ρ . Of course different condensates compete with each other due to the conservation of the density and with evolution of time only one condensate may survive. For long enough times this condensate may achieve 90% of the overall mass in the system. We can observe this behavior in Figure 9.

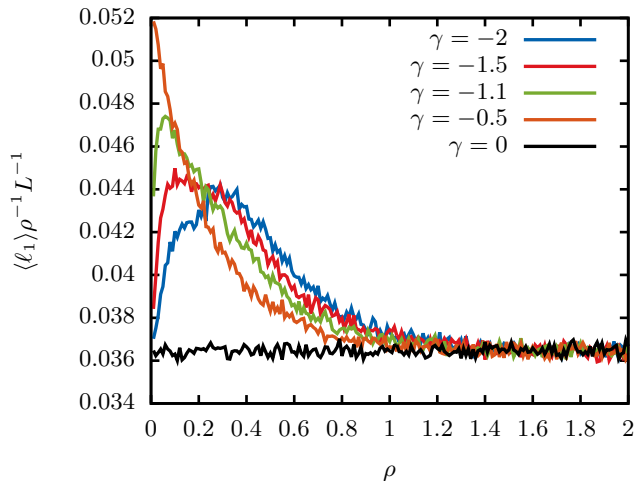


FIG. 10. Mean largest value of the ZRRAP in the stationary limit for different values of γ .

The fluctuations observed early in the system have diminished up to this time point but cannot disappear and in rare cases may lead to the destruction of the condensate. Finally we have to note that this effect accelerates for lower densities.

B. ZRRAP

The truncation of the TARAP analyzed in the last subsection manifests itself in two different ways: the prohibition of transport expressed through the term $(1 - R(m))\delta(r)$ and the reduction of the transported fraction as dictated by the term $\Theta(R(m) - r)$. In order to understand the relevance of these two distinct effects for the condensation mechanics we decided to study two different processes designed according to these terms.

By starting with the first term we arrive at a process which can be regarded as the continuum state space analogue of the zero range process. We will therefore call here this process zero-range random average process (ZRRAP). The fraction density of this process is given by

$$\phi(r|m) = (1 - R(m))\delta(r) + R(m)\Theta(1 - r) \quad (30)$$

with

$$f(m) = \int_0^m d\tilde{m} \int_0^1 dr \phi(r|\tilde{m}) = m. \quad (31)$$

The moments of this density are given by

$$\mu_k = \frac{1}{f(m)} \int_0^1 dr r^k m^{k+1} \phi(r|m) = \frac{m^k}{k+1} R(m). \quad (32)$$

This fraction density describes a process for which with a state-dependent probability the transport rate $r_i(t)$ of

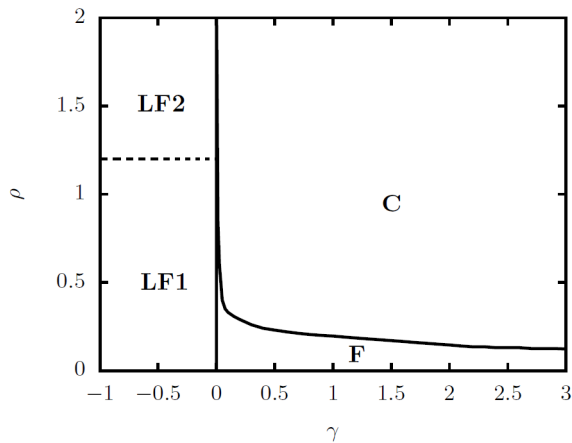


FIG. 11. Phase diagram for the ZRRAP model in the ρ - γ plane for $L = 100$. The dashed line does not correspond to a phase transition but describes the crossover between **LF1-LF2**.

a certain site i at the time point t will be set to 0, while in the complementary event, the rate $r_i(t)$ is randomly distributed with equal probability in the interval $[0, 1]$

For the ZRRAP three different phases can be defined. By choosing $\gamma < 0$ we can see that the mean largest value shows a very interesting behavior, whereas the expected value is always bigger than $0.54 \ln(8.63L + 1)$ for $\rho < 1.2$ (**LF1**). This fact can be observed in Figure 10. Initially a spatial concentration of masses with $m_i > 1$ takes place, which travels through the system unhindered. At the same time the rest of the mass in the system contributes only marginally to the overall flow leading thus to a low-flow phase. This local concentration of mass leads of course to a stationary mean largest value with $\langle \ell_1 \rangle > 0.54 \rho \ln(8.63L + 1)$. For higher densities ($\rho > 1.2$) this effect disappears and the free ARAP-like case is restored (**LF2**).

By studying the system for $\gamma > 0$ we can observe again a fluid and condensate phase as for the TARAP (see Figure 11). There is in general a striking similarity between the two diagrams, which proves the relevance of the restraint on the transition (δ -term in Eq. (26)) for the condensation effect. It is also remarkable that the crossover to the condensate state is more probable in comparison to the TARAP for the same γ . This was to be expected since the condensation dynamics of this system are faster. Fluctuations persist in the system for all parameter values and decrease for increasing values of γ and decreasing densities allowing therefore for a smooth crossover to the stable high flow phase (**F**).

C. SRAP

In the last two subsections we investigated the effect of truncation for fraction densities with a non-zero proba-

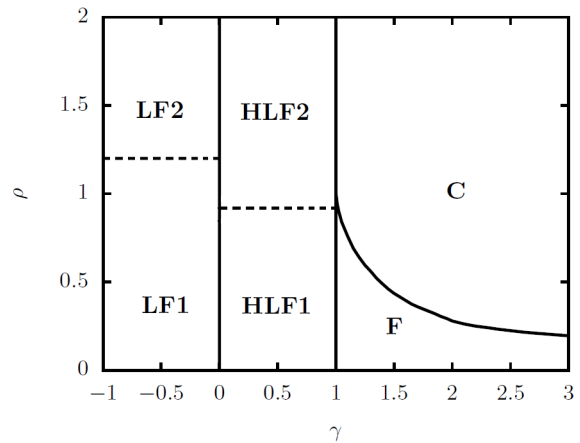


FIG. 12. Phase diagram for the SRAP model in the ρ - γ plane for $L = 100$. The dashed lines do not correspond to a phase transition but describe the crossover between **LF1-LF2** and **HLF1-HLF2** correspondingly.

bility for the event $\{r_i(t) = 0\}$. In this subsection we will show that even for transport processes for which $\{r_i(t) > 0 \forall i, t\}$ holds, a condensate phase appears in the $\rho - \gamma$ plane.

We introduce hereto the fraction density

$$\phi(r|m) = \Theta(R(m) - r) \quad (33)$$

where $\Theta(x_0 - x)$ is the Heaviside function. It is clear that for $\gamma = 0$ the free ARAP model is restored. As before the introduction of the parameter γ allows us to study systems with a large range of moments

$$\mu_k = \frac{1}{f(m)} \int_0^1 dr r^k m^{k+1} \phi(r|m) = \frac{m^k R^k(m)}{k+1} \quad (34)$$

Where we have used the norm

$$\begin{aligned} f(m) &= \int_0^m d\tilde{m} \int_0^1 dr \phi(r|\tilde{m}) \\ &= \int_0^m d\tilde{m} \int_0^1 dr \Theta(R(m) - r) = mR(m). \end{aligned} \quad (35)$$

The phase diagram of this model differs greatly from those of the other two models. We can see that a condensate appears in the system only for $\gamma > 1$. It is especially interesting that in this regime the spatially extended condensate performs a drift through the system. For high values of γ ($\gamma > 1.5$) the position of the condensate stabilizes and the largest value in the system rises up to the stationary value of $0.9\rho L$. Fluctuations are of course present even after the formation of the condensate, but this value remains stationary when integrated over long time-intervals ($T = 10^3$).

For $0 < \gamma < 1$ the flow of the system is below $\frac{\rho}{2}$ while at the same time we can observe a homogeneous mass distribution. We decided therefore to characterize this phase

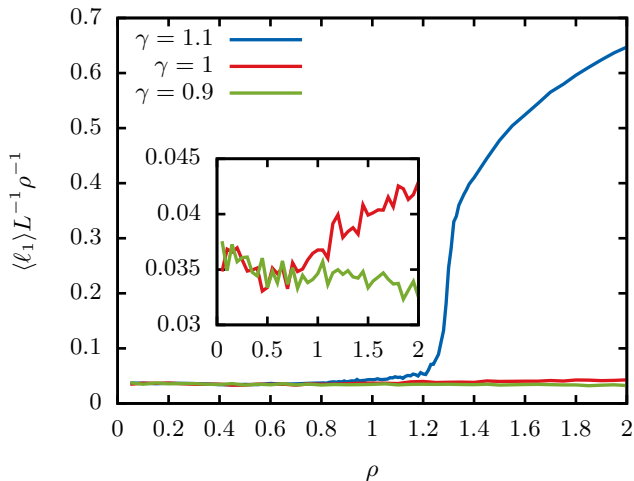


FIG. 13. Mean largest value of the SRAP in the stationary limit for different values of γ .

as homogeneous low flow phase (**HLF**). Surprisingly at first we found out that for $\rho > 0.9$ as shown in Figure 13 the mean largest value in the system decreases with increasing densities (**HLF2**). This discovery is explained by the halt of the drift of the mass due to the truncation effect. Correspondingly we get an equal distribution of the mass and thus a lower mean largest value. This effect does not arise for lower densities and we regain the expected mean largest value of $0.54\rho \ln(8.63L + 1)$ (**HLF1**).

Regarding the $\gamma < 0$ case we have the same structure as described above for the TARAP. For $\rho < 1.2$ we see again a strong fluctuation of the mean largest value with respect to the density. Like in the former processes we can see that these fluctuations disappear for $\rho > 1.2$. It becomes clear that the dynamics of condensation for the TARAP and therefore the transition from fluid to

the condensate phase are controlled by single site fluctuations and consequently by the prohibition of transport (δ - term). At the same time the nature of the phases for $\gamma < 0$ is controlled by collective dynamics and the reduction of the mass transport (Θ - term).

V. CONCLUSION

We analyzed the properties of different truncated random average processes. A convenient choice for the characteristic variable of this system is the largest single-site mass in the system. We derived the distribution of this value which allows us to make some qualitative predictions for the time series of this value. Our results confirm the broken ergodicity property described in [28].

We were able to derive analytical results only in the limit $L \rightarrow \infty$ by studying the order statistics of the system for different lengths, which shows the relevance of this topic for problems of this type. Additionally we introduced the parameter γ allowing us to control effectively the dynamics of the system for finite L . The impact of this parameter on the condensation transition was studied by determining numerically the phase diagram in the $\rho - \gamma$ plane. By comparing the different diagrams we could also clarify the relevance of the different processes like prohibition of transport (δ - term) or reduction of the fraction (Θ - term) for the condensation phase transition.

Interesting generalizations of the presented model may arise. As example one could consider the transport properties of a similar model with open boundary conditions. The performed method could also be useful for other stochastic transport models where a dynamical transition has been observed. Another question that arose during this work and has not yet been answered yet is the behavior of systems with $\gamma = -\infty$. In this case an absorbing stationary state exists in the system and the relation to similar non-equilibrium processes is at hand.

-
- [1] A. Griffin, D. W. Snoke, and S. Stringari, Bose-Einstein Condensation (Cambridge University Press, 1996).
- [2] O. J. O’Loan, M. R. Evans, and M. E. Cates, Psys. Rev. E **58**, 1404 (1998).
- [3] D. Chowdhury, L. Santen, and A. Schadschneider, Phys. Rep. **329**, 199 (2000).
- [4] J. Kaupuzs, R. Mahnke, and R. J. Harris, Phys. Rev. **72**, 056125 (2005).
- [5] P. Bialas, Z. Burda, and D. Johnston, Nucl. Phys. B **493**, 505 (1997).
- [6] P. L. Krapivsky, S. Redner, and F. Leyvraz, Phys. Rev. Lett. **85**, 4629 (2000).
- [7] G. Bianconi and A. L. Barabási, Phys. Rev. Lett. **86**, 5632 (2001).
- [8] J. P. Bouchaud and M. Mézard, Physica A **282**, 536 (2000).
- [9] Z. Burda, D. Johnston, J. Jurkiewicz, M. Kaminski, M. A. Nowak, G. Papp, and I. Zahed, Phys. Rev. E **65**, 026102 (2002).
- [10] K. van der Weele, D. van der Meer, M. Versluis, and D. Lohse, Europhys. Lett. **53**, 328 (2001).
- [11] Satya N. Majumdar, M. R. Evans, and R. K. P. Zia, Phys. Rev. Lett. **94**, 180601 (2005).
- [12] M. R. Evans, S. N. Majumdar, and R. K. P. Zia, J. Stat. Phys. **123**, 357 (2006).
- [13] M. R. Evans and T. Hanney, J. Phys. A: Math. Gen. **38**, R195 (2005).
- [14] M. R. Evans and B. Waclaw, J. Phys. A: Math. Theor. **47**, 095001 (2014).
- [15] S. N. Coppersmith, C.-h. Liu, S. Majumdar, O. Narayan, and T. A. Witten, Phys. Rev. E **53**, 5 4673 (1996).
- [16] R. Rajesh and S. Majumdar, J. Stat. Phys. **99**, 943 (2000).
- [17] J. Krug and J. Garcia, J. Stat. Phys. **99**, 31 (2000).
- [18] F. Zielen and A. Schadschneider, J. Phys. A: Math. Gen. **36**, 13 (2002).

- [19] F. Zielen and A. Schadschneider, *J. Stat. Phys.* **106**, 173 (2002).
- [20] R. Rajesh and S. Majumdar, *Phys. Rev. E* **64**, 036103 (2001).
- [21] J. Cividini, A. Kundu, S. Majumdar, and D. Mukamel, *J. Phys. A: Math. Theor.* **49** (8), 085002 (2016).
- [22] J. Cividini, A. Kundu, S. Majumdar, and D. Mukamel, *J. Stat. Mech.*, 053212 (2016).
- [23] A. Kundu and J. Cividini, *EPL* **115**, 54003 (2016).
- [24] E. Levine, D. Mukamel, and G. M. Schütz, *J. Stat. Phys.* **120**, 759 (2005).
- [25] F. Spitzer, *Adv. Math.* **5**, 246 (1970).
- [26] Y. Sinai, *Lectures in Ergodic Theory* (Princeton University, Princeton, 1977).
- [27] S. Grosskinsky, G. M. Schütz, and H. Spohn, *J. Stat. Phys.* **113**(3/4), 389 (2003).
- [28] F. Zielen and A. Schadschneider, *Phys. Rev. Lett.* **89**, 090601 (2002).
- [29] P. Chleboun and S. Grosskinsky, *J. Phys. A* **48**, 055001 (2015).
- [30] J. Szavits-Nossan, M. R. Evans, and S. N. Majumdar, *Phys. Rev. Lett.* **112**, 020602 (2014).
- [31] S. Chatterjee, P. Pradhan, and P. K. Mohanty, *Phys. Rev. Lett.* **112**, 030601 (2014).
- [32] A. Das, S. Chatterjee, and P. Pradhan, *Phys. Rev. E* **93**, 062135 (2016).
- [33] S. Chakraborti, S. Mishra, and P. Pradhan, *Phys. Rev. E* **93**, 052606 (2016).
- [34] A. Das, A. Kundu, and P. Pradhan, arXiv:1701.05079 (2017).
- [35] S. Majumdar, M. R. Evans, and R. K. P. Zia, *J. Phys. A: Math. Gen.* **37**, 25 (2004).
- [36] M. R. Evans and S. N. Majumdar, *J. Stat. Mech.* P05004 (2008).
- [37] H. A. David, *Order Statistics* (John Wiley and Sons, 1970).